

Cite this: *RSC Mechanochem.*, 2025, 2, 142Received 24th September 2024  
Accepted 4th November 2024

DOI: 10.1039/d4mr00110a

rsc.li/RSCMechanochem

# Shaking up conjugates between chitosan and aldehydes *via* mechanochemistry†

Casper Van Poucke,  Sven Mangelinckx  and Christian V. Stevens \*

A solid-state mechanochemical protocol to synthesize Schiff base and *N*-alkyl chitosan derivatives is described. The transition from a liquid reaction medium to a solid-state reaction allowed for a more efficient conjugation between the added hydrophobic aldehydes and hydrophilic chitosan by circumventing the generally observed solubility mismatch. Furthermore, for the reductive amination, the utilization of NaBH<sub>4</sub> was facilitated instead of NaCNBH<sub>3</sub>. The overall sustainable character of the reaction was compared to other solution-based methods *via* the calculation of the RME and PMI green metrics.

## Introduction

Chitosan and its many derivatives, produced from widely available chitin found in the exoskeletons of insects and crustaceans or the cell walls of fungi and microorganisms, have emerged as a versatile and environmentally friendly class of biopolymers with a broad range of applications. These biobased polymers have gained increasing attention due to their unique properties and wide-ranging uses across various industries.

Two interesting classes of chitosan derivatives are the *N*-alkyl and the *N*-alkylidene chitosans, which enhance the versatility of chitosan by altering its innate hydrophilic-lipophilic balance (HLB), making it suitable for applications demanding specific hydrophobic properties. *N*-Alkylidene chitosan derivatives can be utilized as corrosion inhibitors on metallic surfaces,<sup>1</sup> as antimicrobial agents,<sup>2</sup> as low-cost oil adsorbents for the removal of crude oil spills<sup>3</sup> and even as controlled release systems of bioactive aldehydes.<sup>4,5</sup> The reversible nature of the imine moiety under acidic aqueous conditions, although unimportant or beneficial for certain applications as listed above, might be problematic for certain other applications as the formed aldehydes readily leach from the obtained materials. To address this problem, the imine can be reduced to the corresponding amine. The produced *N*-alkyl chitosan derivatives find applications as agents to impart surface hydrophobicity to wood or paper, thereby enhancing water resistance.<sup>6,7</sup> Moreover, *N*-alkyl chitosans have recently proven to be effective within the bio-flocculation of microalgae,<sup>8</sup> the formation of non-toxic biomedical hydrogels<sup>9</sup> or as drug delivery agents.<sup>10</sup> Yet, despite the broad potential applicability of *N*-alkylidene and *N*-alkyl chitosans, their efficient and effective synthesis remains challenging. *N*-alkylidene chitosan derivatives (often called

chitosan Schiff bases) are mostly synthesized *via* the mixing of chitosan with the corresponding aldehyde utilizing either acidic water, ethanol, methanol or combinations thereof as a solvent under heterogeneous or homogeneous conditions. The *N*-alkyl chitosan derivatives on the other hand are predominantly synthesized *via* an aqueous one-pot reductive amination,<sup>11,12</sup> as the reaction proceeds homogeneously while *N*-selectivity is assured. Remarkably, both these reactions are mainly limited by the inherent reactivity and incompatibility of the added reactants with the utilized solvents, as chitosan does not dissolve in alcohols and the employed hydrophobic aldehydes are often completely water-insoluble. Additionally, in the case of *N*-alkyl chitosans, problematic reducing agents like NaCNBH<sub>3</sub> are required to selectively reduce the formed iminium intermediates under aqueous acidic conditions. However, under these reaction conditions, as well as during the workup, toxic hydrogen cyanide can be produced, making the scale-up beyond the laboratory scale problematic.

Within this study, for the first time, solid-state synthesis of *N*-alkylidene and *N*-alkyl chitosan derivatives *via* mechanochemistry is explored as a green and more effective alternative. This allowed for the complete elimination of solvents during the synthesis of both classes of compounds as well as a major reduction in the required solvent during product isolation and purification. The more sustainable character was further evidenced by the process mass intensity (PMI) and reaction mass efficiency (RME) green metrics. Furthermore, the protocol allowed for an easy swap towards biobased aldehyde feedstocks of which citronellal and 5-substituted furfurals were utilized as model substrates. Moreover, for the synthesis of *N*-alkyl chitosan derivatives, the less problematic NaBH<sub>4</sub> and  $\alpha$ -picoline borane complex (PICB) could be utilized instead of NaCNBH<sub>3</sub>.

## Safety notice

When performing mechanochemical reactions with borohydrides in a ball mill, safety precautions should be taken. Within

Department of Green Chemistry and Technology, Faculty of Bioscience Engineering, Ghent University, Coupure Links 653, B-9000 Ghent, Belgium. E-mail: chris.stevens@ugent.be

† Electronic supplementary information (ESI) available. See DOI: <https://doi.org/10.1039/d4mr00110a>



this study, reactions were performed in a well-ventilated fume hood and after the reaction, the mill was allowed to cool down for one hour after which the jars were removed wearing a face shield.

Although no incidents occurred during this study at a 500 mg chitosan scale, borohydrides are known to decompose in contact with the moisture from the air, with the formation of hydrogen gas, which could spontaneously ignite upon impact within the stainless steel jars. An inert atmosphere is recommended if a scale-up of these reactions would be required, as demonstrated by Isoni *et al.*<sup>13</sup>

## Neat mechanochemical chitosan Schiff base formation

Inspired by chitosan's natural fat-encapsulating properties, which have enabled its exploitation as a dietary supplement for the past 20 years,<sup>14</sup> together with the well-established neat mechanochemical synthesis of imine covalent organic frameworks (COFs),<sup>15</sup> it was hypothesized that the reaction between chitosan and water-insoluble aldehydes, towards the respective imine, should proceed readily under neat mechanochemical conditions.

Given our previous experience with the solution-based synthesis of these compounds,<sup>16</sup> octanal was selected as an initial benchmark of a general water-insoluble linear aldehyde. Therefore, the mechanochemical reaction between chitosan and 0.625 equivalents of octanal was monitored qualitatively by FTIR analysis (see Fig. 1). After 30 seconds of milling no significant reaction could be observed, indicated by the presence of the characteristic  $\text{CaO}$  stretch at  $1726\text{ cm}^{-1}$  and the  $\text{H}-\text{CaO}$  stretch at  $2713\text{ cm}^{-1}$  of the original aldehyde, together with the  $\text{NH}_2$  scissoring vibration at  $1583\text{ cm}^{-1}$  of chitosan. However, after 10 minutes of milling full conversion could be observed *via* FTIR as both signals at  $1726$  and  $2713\text{ cm}^{-1}$  disappeared. Additionally, there was a reduction in the signal at  $1583\text{ cm}^{-1}$  and a new  $\text{CaN}$  stretch at  $1668\text{ cm}^{-1}$  appeared, both

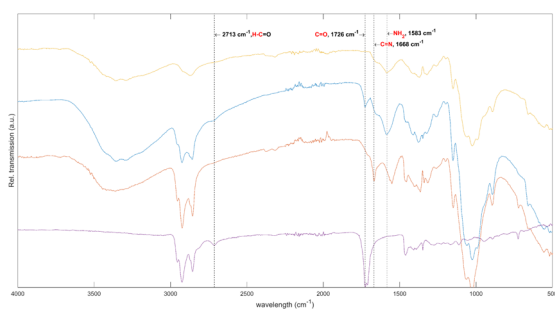


**Fig. 1** Comparison between the FTIR spectrum of chitosan (yellow), chitosan + 0.625 eq. octanal after 30 seconds of milling (blue), chitosan + 0.625 eq. octanal after 10 minutes of milling (orange) and octanal (purple). The  $\text{CaO}$  stretch at  $1726\text{ cm}^{-1}$  and  $\text{H}-\text{CaO}$  stretch at  $2713\text{ cm}^{-1}$  of the original aldehyde, the  $\text{NH}_2$  scissoring vibration of chitosan at  $1583\text{ cm}^{-1}$  and the newly formed  $\text{CaN}$  imine stretch at  $1668\text{ cm}^{-1}$  of the product are indicated with a dotted line. A 25 mL SS jar containing 500 mg chitosan was utilized together with two 15 mm SS balls at a frequency of 30 Hz.

indicative of *N*-octylidene formation.<sup>17</sup> Moreover, the obtained reaction product became completely water-insoluble, even under acidic conditions. However, despite the initial success, from an environmental standpoint, the utilization of natural aldehyde feedstocks, such as natural essential oils over their petrochemical-derived equivalents is preferred. To this extent, citronellal was subsequently utilized as a model compound.

Chitosan was reacted with different amounts of citronellal and the reaction was monitored *via* FTIR. Additionally, to quantify the obtained degree of substitution *via* elemental analysis ( $\text{DS}_{\text{EA}}$ ), the samples were purified by soaking them in ethanol until no aldehyde signals could be observed *via* FTIR (see Fig. S1–S4 and S6†). Afterward, they were dried and analyzed (see Table S2†). Based on these results, the degree of substitution ( $\text{DS}_{\text{EA}}$ ) and reaction mass efficiency ( $\text{RME}_{\text{EA}}$ ) were calculated which are depicted in Fig. 2. When 0.125 or 0.250 equivalents of citronellal were added, complete conversion was observed after 10 minutes with a  $\text{DS}_{\text{EA}}$  of 4.5 and 11.7% and a  $\text{RME}_{\text{EA}}$  of 39.1 and 50.9%, respectively. When 0.5 equivalents were added the required time until the aldehyde signals completely disappeared increased to 30 minutes (see Fig. S3†), resulting in a  $\text{DS}_{\text{EA}}$  of 31.2% and a  $\text{RME}_{\text{EA}}$  of 67.8%. The discrepancy between the obtained  $\text{DS}_{\text{EA}}$  and the observed full FTIR conversion is something we do not have an explanation for at the moment. However, we believe that the relative sensitivity of the FTIR apparatus might be a part of the answer, which will be studied in the future. Moreover, when one equivalent of citronellal was added, no full conversion could be observed after 40 minutes of milling (see Fig. S4†) while the obtained  $\text{DS}_{\text{EA}}$  and  $\text{RME}_{\text{EA}}$  dropped to 14.5% and 15.8%, respectively. This is most likely due to the high liquid-to-solid ratio of the reaction mixture ( $\eta = 0.95$ ), making it more of a slurry rather than a homogeneous powder. Subsequently, the transfer of mechanical energy from the system to the reaction mixture remained limited. To try to alleviate this problem, two different approaches were examined, both aimed at improving the overall rheology of the reaction mixture during milling. On the one hand, NaCl was added as a solid grinding auxiliary together with 1 equivalent of citronellal. On the other hand, 1 equivalent

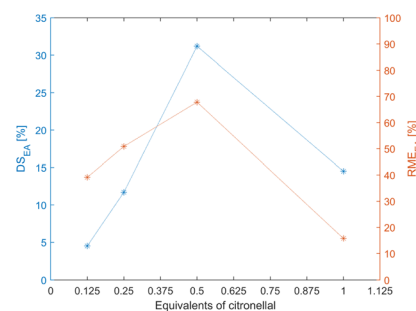


**Fig. 2** The calculated degree of substitution of the formed Schiff base ( $\text{DS}_{\text{EA}}$ ) and reaction mass efficiency ( $\text{RME}_{\text{EA}}$ ) based on elemental analysis (EA) in function of the added equivalents of citronellal. The chitosan mass within the system was kept constant at 500 mg. A 25 mL SS jar was utilized together with two 15 mm SS balls at a frequency of 30 Hz. The dotted lines connect the different data points and are only added as a guide to the eye.



of citronellal was added in portions of 0.25 equivalents every 10 minutes. Both methods were monitored *via* FTIR (see Fig. S5 and S6†) and after 60 minutes of milling, they gave an exceptionally high  $DS_{EA}$  of  $\sim 100\%$  (measured 101.1%) and 94.8%, respectively. However, the addition of NaCl lowered the overall reaction rate, as it diluted the reaction mixture. When looking at these results, comparably low conversions are reported in aqueous acidic solutions, both for aromatic and aliphatic aldehydes, which never exceed a conversion of 12% despite adding 2 equivalents of aldehyde.<sup>18</sup> Under mechanochemical conditions, the polarity mismatch between chitosan and the employed aldehydes is no longer a problem<sup>19</sup> and water formed during the reaction easily evaporates as the particle size gets reduced and the available surface increases. This phenomenon can be observed visually as the reaction mixture goes from a paste-like substance to a fine free-flowing powder throughout the reaction.

## Mechanochemical reductive amination

Certain applications require a balance between the added hydrophobicity by the *N*-alkyl group and the subsequent acidic aqueous solubility of the obtained derivative. As for these types of applications, the aqueous solubility is crucial for the proper functioning of the chitosan derivative, limiting the maximum allowed DS. Examples are viscosity modifiers,<sup>11</sup> emulsifiers,<sup>20</sup> algal flocculants<sup>8</sup> and antimicrobial agents. However, chitosan Schiff bases are prone to hydrolyze under aqueous acidic conditions, especially when dissolved.<sup>4</sup> A possible solution is the reduction of the obtained imine towards the corresponding lowly substituted amine as numerous described before in solution. However, we wanted to check whether the subsequent reduction of the obtained imine could also be facilitated *via* a one-pot solid-state reaction under vibrational milling. To the author's knowledge, the mechanochemical reductive amination of chitosan has not been described before.† However, there are three recent examples of mechanochemical reductive aminations employed to synthesize small molecules.<sup>21–23</sup>

As an initial starting point, our optimal conditions for the liquid phase reaction, as previously described<sup>16</sup> but without solvent, were utilized in a one-step mechanochemical reaction (pathway B in Fig. 3). A  $DS_{NMR}$  of 4.2% was obtained, which is close to our previously obtained  $DS_{NMR}$  of 5% utilizing these conditions in the liquid phase.<sup>16</sup> A second experiment involved

† This was true at the time this article was originally submitted. However, during revisions, an article was published by Yang *et al.*<sup>41</sup> which covered a similar scope with some overlapping findings. When we applied their proposed methodology, a DS of about 75% was obtained for *N*-(furan-2-yl)methyl chitosan. This is higher than the value obtained with the methodology proposed within this article but requires a total reaction time of more than 3 days when aging is included. Moreover, in their article, low degrees of substitution are reported for fatty aldehydes with more than eight carbon atoms, which they attributed to potentially poor diffusion of the aldehyde onto the chitosan chain. However, as indicated above, chitosan has found applications as a fat-encapsulation agent. Therefore, we propose that this might be related to the overall rheology of the reaction mixture instead, which could be alleviated by the addition of a solid grinding auxiliary as shown above (*vide infra*).

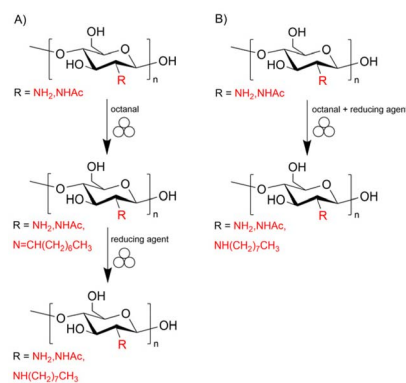


Fig. 3 Graphical representation of the one-step (B) and two-step (A) protocol utilized to synthesize *N*-octyl chitosan.

Schiff base formation before the addition of the reducing agent, as the mechanochemical setup allowed for easy separation in time between the condensation and reduction *via* a two-step procedure (pathway A in Fig. 3). This yielded an improved DS of 5.9%. Next, a two-fold increase in the added amount of reducing agent was applied to check whether the reaction would proceed faster. This resulted in only a 1.6% increase in  $DS_{NMR}$  up to 7.5% (see entry 4 Table 1). Subsequently, as described by Canale *et al.*,<sup>22</sup> liquid-assisted grinding (LAG) utilizing acetic acid ( $\eta = 0.2$ ) was applied to the two-step protocol. However, no improvement in  $DS_{NMR}$  could be observed (see entry 3 Table 1). A change of reducing agent from the preferred PICB to the more problematic NaCNBH<sub>3</sub> did not change the obtained  $DS_{NMR}$  either. This further inspired us to use the less selective and more reactive NaBH<sub>4</sub> as the reaction now proceeds in two distinct steps through the intermediate imine. Much to our delight, the reaction proceeded as before, indicating that the added reducing agent no longer needs to be tempered when the reaction proceeds in two distinct steps. This further implies that

Table 1 Overview of the different applied reaction conditions and their effect on the degree of substitution ( $DS_{NMR}$ , calculated based on <sup>1</sup>H NMR) of the obtained product

Entry	Reaction <sup>a</sup>	Reducing agent [eq.]	$DS_{NMR}$ [%]
1	Two-step	PICB (0.1)	5.9
2	One step	PICB (0.1)	4.2
3	Two-step, LAG	PICB (0.1)	6.0
4	Two-step	PICB (0.2)	7.5
5	Two-step	NaCNBH <sub>3</sub> (0.1)	5.9
6	Two-step	NaBH <sub>4</sub> (0.1)	6.0
7	Liquid phase reaction <sup>16</sup>	PICB (0.1)	5

<sup>a</sup> A 25 mL SS jar containing 500 mg chitosan and 51.4  $\mu$ L octanal (0.125 eq.) was utilized together with two 15 mm SS balls at a frequency of 30 Hz for all reactions. For the two-step protocol, chitosan and octanal were milled for 10 minutes. Afterward, the reducing agent was added and the mixture was milled for another two hours. This was in contrast with the one-step protocol in which everything was added and the mixture was milled for two hours. For the two-step LAG protocol, the acetic acid ( $\eta = 0.2$ ) was added together with the reducing agent. The absence of boron salts in the obtained products after purification was verified by <sup>11</sup>B NMR.



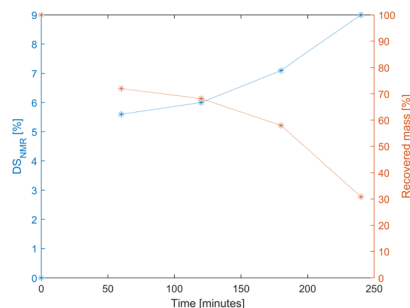


Fig. 4 The degree of substitution ( $DS_{NMR}$ , calculated based on  $^1H$  NMR) and the percentage of mass that was recovered after the reaction in function of time. The previously explained two-step protocol utilizing  $NaBH_4$  (see entry 6 Table 1) was utilized for all reactions. The dotted lines connect the different data points and are only added as a guide to the eye.

$NaBH_4$  no longer needs to be derivatized with big toxic tempering groups like cyanides or pyridine derivatives, which severely improves the atom economy of the reaction as well as the overall process safety.

Finally, for the best conditions selected above (see entry 6 Table 1), the obtained  $DS_{NMR}$  and the recovered m% of chitosan were monitored in time. As depicted in Fig. 4, the obtained  $DS_{NMR}$  increased with time while the % recovered mass sharply decreased after 180 and 240 minutes of milling. This sharp decrease in mass can be explained by the extensive cleavage of glycosidic bonds within the polysaccharide backbone due to the prolonged stress imposed by the milling system at longer reaction times (see Table S1 and Fig. S21†).<sup>24,25</sup> These produced short-chain fragments are lost during product purification as they dissolve upon washing the obtained product with water (see Experimental section). To further verify this hypothesis, chitosan itself was milled for two hours, with the recovery of about 75% of the chitosan mass afterward, which is very close to the observed recovery of 68% after two hours of reaction. This degradation can potentially be lowered by utilizing different configurations that lower the mechanical energy that is supplied to the system, by for example the utilization of smaller milling balls or different milling materials. Based upon the observations above, the reaction time was kept at 120 minutes as this was the optimal compromise between sufficient derivatization and product recovery afterward.

Until now, only lowly substituted *N*-alkyl chitosan derivatives that remain soluble under aqueous acidic conditions were examined. However, in some cases, acidic aqueous solubility is of less concern or even undesired. An example is their application as water-resistant coatings, as a certain hydrolytic resistance is desired in this case. To this extent, the influence of the added equivalents of aldehyde and reducing agent on the obtained DS, beyond water-soluble *N*-alkyl chitosan derivatives, was evaluated. As in theory, any solubility mismatches could be omitted *via* solid-state synthesis. As indicated by Fig. 5, the calculated DS (both based on  $^1H$  NMR and EA) increases with the amount of equivalents of aldehyde added, yet the reaction never goes towards completion within 120 minutes, while the

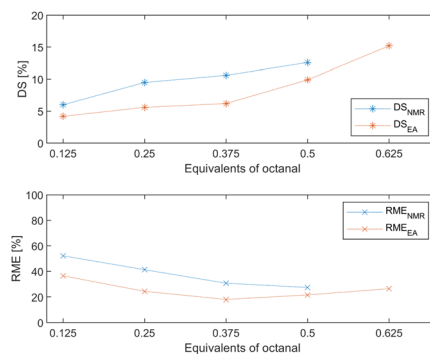


Fig. 5 The calculated degree of substitution (DS) and reaction mass efficiency (RME) based on elemental analysis (EA) and  $^1H$  NMR analysis in function of the added equivalents of octanal. At 0.625 equivalents of octanal, the product no longer dissolved under aqueous acidic conditions, so no liquid phase  $^1H$  NMR analysis could be conducted. The same octanal to  $NaBH_4$  ratio of 0.125/0.1 was utilized in all experiments. The dotted lines connect the different data points and are only added as a guide to the eye.

reagent utilization (RME) decreases. This indicates the potential need for longer milling times. However, this will be at the cost of the amount of mass that can be recovered afterward (*vide supra*). Overall, the reduction of the imine seems to be the rate-limiting step as it is a lot slower under these mechanochemical conditions compared to the imine formation. Hence, another potential way of increasing the amount of recovered mass, in some cases, might be the direct utilization of highly modified *N*-alkylidene chitosan derivatives instead.

Subsequently, as for the Schiff base formation, octanal was replaced by citronellal as a more durable aldehyde feedstock. Resulting in a  $DS_{NMR}$  of 10.9% based on  $^1H$  NMR analysis (6% based on EA analysis) with 0.125 equivalents of citronellal added, doubling the obtained degree of substitution compared to the  $DS_{NMR} = 5\%$  obtained *via* the liquid phase reaction.<sup>16</sup> Another important advantage is the ease of product isolation, as only water and ethanol washes are required. This is in strong contrast with our previous liquid phase reaction where a large volume of acetone was required for product precipitation and subsequent isolation. This will be further discussed in the section Green metrics. Additionally, during the required acidic quench of PICB at 60 °C in the liquid phase protocol, the prenyl group of the attached side chain got partially hydrated, as evidenced by the three different methyl groups (8', 8'' and 9'') in Fig. 6. This is in contrast with the mechanochemical reaction, as the prenyl group remained completely intact, reflected by the two large signals of the methyl groups (8'' and 9'') and one methine group (6'') in Fig. 6, as this quench was no longer required. The findings above indicate the possibility of directly utilizing aldehyde-containing essential oils, without aldehyde isolation, as in the work of Paula *et al.*<sup>26</sup> This, because all unreacted and non-aldehyde-containing components could be easily removed afterward *via* washing of the obtained product.

Finally, the solid-state reductive amination between furfural or furfural-like derivatives and chitosan was explored, as these substrates form another important class of bio-derived



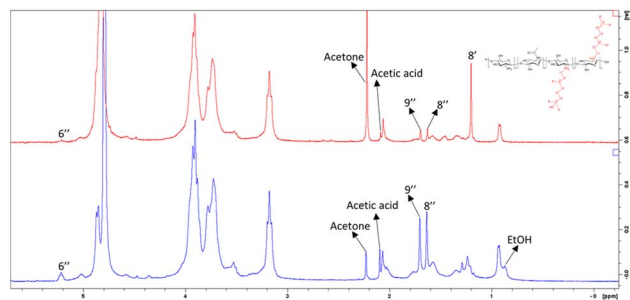


Fig. 6 Comparison between the  $^1\text{H}$  NMR spectrum (400 MHz at  $20\text{ mg mL}^{-1}$  in 1 vol% d-TFA in  $\text{D}_2\text{O}$ ) obtained via the liquid phase reaction (red) and the solid phase reaction (blue). The reaction conditions applied for the liquid phase reaction can be found in ref. 19. The reaction conditions for the solid phase reaction are the same as in entry 6 of Table 1.

aldehydes, while the cycloaddition products of *N*-(furan-2-yl) methyl chitosan and bis-maleimide crosslinkers have been extensively studied for their applications in biomedical hydrogels.<sup>9,27</sup> To this end, six commercially available 5-substituted furfural derivatives were selected, as they allowed for the study of electronic effects and the aggregation state of the added aldehyde on the obtained  $\text{DS}_{\text{NMR}}$ . Moreover, to check the generality of the proposed mechanochemical protocol, the scope was further expanded with two furfural-like derivatives containing a thiophene and pyrrole core, respectively.

First, the protocol was tailored to accommodate these new aldehyde substrates. The required reaction time for sufficient Schiff base formation, while avoiding excessive milling times (*vide supra*), was determined *via* FTIR analysis of the model reaction between chitosan and one equivalent of furfural (see Fig. S9<sup>†</sup>). A reaction time of 30 minutes was selected, while the reaction time of the subsequent reduction was kept at 120 minutes (*vide supra*). Subsequently, the product isolation was optimized as these resonance-stabilized aromatic imines required a dissolution in 1% (v/v) acetic acid to be efficiently removed (see Fig. S10 and S11<sup>†</sup>).

After adapting the protocol, the remaining eight substrates were tested. The Schiff base formation was monitored *via* FTIR after 10 and 30 minutes of milling for all reactions. In general, the observed conversion of the starting aldehyde towards the Schiff base correlated well with the final obtained  $\text{DS}_{\text{NMR}}$  of the product (see Fig. S9–S20<sup>†</sup>). Consequently, this FTIR-monitored conversion can be utilized as an early indicator of the potential reaction outcome.

Six furfural and furfural-like derivatives could be reductively aminated onto chitosan with a modest to high  $\text{DS}_{\text{NMR}}$  (see entries A–C, E and H–I in Table 2). However, three other entries were not successful. Firstly, the obtained product in entry D was deborylated despite a successful reductive amination, as seen in Fig. S15.<sup>†</sup> For entry F, a strong exotherm was observed during the reduction of the Schiff base, which completely charred the resulting material. Additionally, 5-(4-nitrophenyl)furfural showed no reactivity, during Schiff base formation or the

Table 2 Overview of the different utilized furfural and furfural-like derivatives and the degree of substitution ( $\text{DS}_{\text{NMR}}$ , calculated based on  $^1\text{H}$  NMR) of their respective products, together with the aggregation state of the aldehyde and the *para* Hammett constants for the respective substituents

Entry	Aldehyde	$\text{DS}_{\text{NMR}}$ [%]	Aggregation state	Hammett constant ( $\sigma_p$ ) <sup>31</sup>
A		55.9	Liquid	0
B		56.6	Liquid	-0.17
C		42.2	Crystalline solid	0.23
D		19.7 <sup>a</sup>	Solid	0.12
E		64.4	Solid <sup>b</sup>	0
F		— <sup>c</sup>	Solid	0.78
G		N.R.	Solid	0.25
H		42.0	Liquid	—
I		11.0	Crystalline solid	—

<sup>a</sup>  $\text{DS}_{\text{NMR}}$  of the deborylated product. <sup>b</sup> Added as a 95 m% slurry in water. <sup>c</sup> A strong exotherm was observed during the reduction of the formed Schiff base which completely charred the resulting material.



subsequent reduction step, as seen in entry G of Table 2 and Fig. S18.† Moreover, no clear relationship was observed between the Hammett constants of the substituents and the observed  $DS_{\text{NMR}}$ . Furthermore, the aggregation state of the aldehyde by itself did not seem to explain the observed reactivity either, as solid and liquid aldehydes gave similar results (entries A, B and E for example). The solid-state reactivity is most likely governed by a combination of a rheological and chemical factor, as shown in the work of Vugrin *et al.*<sup>28</sup> However, for crystalline solids such as 5-bromofurfural in entry C, a reduction in crystallinity could be observed during milling, which is assumed to be accompanied by an increased reactivity over time (see Fig. S13†). Additionally, as demonstrated above, the polarity mismatch between chitosan and the utilized hydrophobic aldehydes, such as 5-bromofurfural or thiophene-2-carboxaldehyde, did not pose any problem (*vide infra*). Furthermore, the synthesized *N*-(thiophen-2-yl)methyl chitosan showed an interesting peak broadening of the aromatic signals within the  $^1\text{H}$  NMR spectrum, indicative of  $\pi$ - $\pi$  stacking, similar to other thiophene-containing polymers which might find application in optoelectronics<sup>29</sup> (see Fig. S24†), while the thiophene core itself presents opportunities for applications as selective metal adsorbents.<sup>30</sup>

## Green metrics

Firstly, as an initial indication of the overall performance of our system towards the synthesis of *N*-alkylidene chitosan derivatives, the reaction mass efficiency (RME) (eqn (1)) was compared to two recent alternative syntheses and one solvent-based method. The RME can be defined as the percentage of the reagent that ends up on the chitosan chain (see Experimental section). The RME indicator was selected as an early indicator as most protocols lacked sufficient data to calculate an overall PMI for example. Some protocols involved the utilization of citral as an aldehyde source while others utilized citronellal (see Table 3). However, due to their strong structural similarity, only differing in the amount of saturation, the systems were deemed comparable. The first system developed by Sela *et al.*<sup>32</sup> utilized a continuous solvent-free synthesis in which a major excess of aldehyde was utilized to ensure proper mixing between the chitosan particles and the reaction medium. Afterward, the modified chitosan particles were separated and the medium was reused. The second protocol by Marin *et al.*<sup>18</sup> involved a more classical approach, as chitosan was dissolved under acidic aqueous conditions, after which the respective aldehyde

**Table 3** Overview of the calculated degree of substitution (DS) and reaction mass efficiency (RME) of several different studies involving the synthesis of *N*-alkylidene chitosan derivatives. The calculations of the RME can be found in the ESI

	Sela <i>et al.</i> <sup>32</sup>	Marin <i>et al.</i> <sup>18</sup>	Lin <i>et al.</i> <sup>5</sup>	Our work
Aldehyde	Citral	Citral	Citronellal	Citronellal
DS [%]	3.1	52.7	85.7	100 <sup>a</sup>
RME [%]	0.84	62.0	20.1	100 <sup>a</sup>

<sup>a</sup> Measured 101.1%.

was added and left to react. Afterward, all volatile compounds were removed to isolate the product. The final solvent-based method from Lin *et al.*<sup>5</sup> involved the dispersion of chitosan particles in a methanol solution containing the aldehyde.

Although very innovative, the method by Sela *et al.*<sup>32</sup> scored poorly with an RME of below 1%, as in the end only a low fraction of the aldehyde gets attached to the chitosan chain, while a lot of the reactant gets lost during the separation. However, the authors did provide a proof of concept and in the future different types of setups could further improve this system. The system by Lin *et al.*<sup>5</sup> scored moderately with an RME of 20.1%, yet they were able to reach a high degree of substitution. Finally, the system of Marin *et al.*<sup>18</sup> had a high RME of 62.0% and an intermediate DS of 52.7%. Comparing all these systems to our system, which had the highest DS and RME overall, the advantages of mechanochemistry in this case are evident. However, it must be noted that these metrics do not take into account the fact that a certain mass fraction will be lost due to degradation upon extensive milling. Moreover, both the system of Lin *et al.*<sup>5</sup> and Marin *et al.*<sup>18</sup> required large amounts of solvent in their synthesis, which was also not considered in this initial assessment. To take these into account, another indicator like the PMI, for example, could be utilized. However, insufficient data was available to do so. When looking at the data below for the reductive amination, as well as previously obtained data by our group<sup>25</sup> on a similar scale, a decrease in the PMI related to the synthesis of these compounds with a factor of 100 could be expected.

For the synthesis of *N*-alkyl chitosan derivatives,  $\text{NaBH}_4$  was selected as the reducing agent of choice. Firstly, three pre-selected potential reducing agents were ranked based on their overall “greenness” by the GSK reagent selection guide for reductive aminations.<sup>33</sup> Based on these scores,  $\text{NaCNBH}_3$  was excluded, while  $\text{NaBH}_4$  had a similar score to PICB (see Table 4). Within the selection guide, the reagent atom efficiency was approximated by the reagent molecular weight ( $M_w$ ). This is a reasonable assumption as all three reagents are equivalent to one hydride (or in the best case three or four), while the rest of the reagent's mass can be regarded as waste from a chemical standpoint. Yet, within the guide, all compounds with a reagent mass below  $140 \text{ g mol}^{-1}$  scored equally well and received a maximum score. Based on the reasoning above, this is quite counterintuitive, as the mass of PICB is a factor three higher than  $\text{NaBH}_4$ , resulting in three times as much generated waste. This waste is not only bad from an environmental standpoint but also from an economic perspective, as more reagent will be required in the first place to facilitate the same transformation.

Next, the process mass intensity (PMI) (eqn (2)) of our mechanochemical protocol was benchmarked against our own

**Table 4** Overview of the GSK “Greenness” score and the reagent's molecular weight

	$\text{NaBH}_4$	$\text{NaCNBH}_3$	PICB
GSK “Greenness” score	6.4	2.7	6.6
$M_w$ ( $\text{g mol}^{-1}$ )	37.83	62.84	106.96



**Table 5** Overview of the calculated degree of substitution ( $DS_{\text{NMR}}$ ) and process mass intensity (PMI) of different studies involving the synthesis of *N*-octyl chitosan derivatives. The calculations of the PMI can be found in the ESI<sup>a</sup>

	Desbrières <i>et al.</i> <sup>11</sup>	Van Poucke <i>et al.</i> <sup>16</sup>	This work
$DS_{\text{NMR}}$ [%]	12.5	5	5.5
$PMI_{\text{reaction}}$	80.4	97.8	1.73
$PMI_{\text{isolation}}$	N.D	234.9	139.8
PMI	N.D	332.7	141.5

<sup>a</sup> N.D = no data reported.

previously optimized solution-based protocol<sup>16</sup> as well as the most adapted procedure in the literature by Desbrières *et al.*<sup>11</sup> to produce lowly substituted *N*-alkyl chitosan derivatives (see Table 5).

As previously observed,<sup>25</sup> switching to a mechanochemical process resulted in about a 100-fold reduction in  $PMI_{\text{reaction}}$ , compared to both solvent-based methods, as there is no longer any solvent required during the reaction. Additionally, compared to our previous work,<sup>16</sup> the  $PMI_{\text{isolation}}$  could be reduced by a factor of 1.7, while the utilized MeOH and acetone could be replaced by the more recommended EtOH and water, according to the CHEM21 solvent selection guide.<sup>34</sup> For the whole process, the PMI could be reduced by a factor of two, effectively cutting the amount of generated waste in half. Unfortunately, the isolation step could not be compared with the work of Desbrières *et al.*<sup>11</sup> as no sufficient data was supplied regarding the product isolation. However, the PMI of the overall process is expected to be similar or higher compared to our solvent-based process as the isolation included several poorly documented washing steps. Finally, to check the performance of the mechanochemical protocol on a bigger scale, the reaction towards *N*-(furan-2-yl)methyl chitosan was repeated five times and the whole batch of replicates was subjected to one combined work-up. This combined approach was compared to the work-up of one single run. For the 500 mg scale single run, a  $PMI_{\text{reaction}}$  of 2.77 and  $PMI_{\text{isolation}}$  of 209.8 were obtained. In contrast, when the isolation of five runs was combined, a similar  $PMI_{\text{reaction}}$  of 2.72 was attained, while the  $PMI_{\text{isolation}}$  was decreased by a factor of 1.7 (to 123.1). This reduction could be ascribed to the minimization of unavoidable losses during isolation.

## Conclusion

Within this study, mechanochemistry was successfully applied to synthesize two classes of hydrophobic conjugates between chitosan and aldehydes *via* either a solid-state Schiff base formation or a solid-state reductive amination, resulting in *N*-alkylidene and *N*-alkyl chitosan derivatives, respectively. The solid-state mechanochemical reductive amination allowed for easy separation (in time) of the imine formation and subsequent reduction which in turn allowed for the utilization of  $\text{NaBH}_4$  as a reducing agent. Additionally, the solid-state protocol significantly simplified the purification of most

products, requiring only minimal washing with water and ethanol, without the need to neutralize any residual  $\text{NaBH}_4$  under aqueous acidic conditions. This is particularly advantageous for acid-sensitive products such as citronellal. However, for the isolation of furfural and furfural-like chitosan derivatives, dissolution was still required after water washing due to the formation of more stable aromatic imines. Nevertheless, when the purification was carried out on a bigger scale, the overall PMI could be reduced by a factor of two. Moreover, contrary to solution-based approaches, solid-state amination and Schiff base formation both allowed for the efficient utilization of natural aldehydes and other hydrophobic substrates with opposite polarity to chitosan. Overall, both mechanochemical methods exhibited promising potential and favorable performance compared to conventional methods, as indicated by the RME and PMI green metrics. Another major advantage is the possibility of transferring the system from batch mode through ball milling toward a continuous process *via* reactive extrusion.<sup>35,36</sup> This will enable the high-volume production and application of these types of chitosan derivatives of the future, aiding in the transition toward a sustainable tomorrow.

## Experimental

### Materials

All chemicals and reagents were commercially available and obtained in analytical purity or higher from Tokyo Chemical Industry Co., Sigma-Aldrich and Carl Roth. Low molecular weight chitosan (KitoGreen®) ( $M_w$  = see Table S1,† DA = 0.08, origin = fungal, 5.27 mmol  $\text{NH}_2$  per gram, insoluble fraction: 12–15 m% chitin-glucan complex, water content =  $8.4 \pm 0.2\%$ ) was supplied by KitoZyme (Herstal, Belgium) and utilized without further purification. The DA was determined based on  $^1\text{H}$  NMR.<sup>37</sup> The amount of reactive  $\text{NH}_2$  units in a gram of material was determined *via* an average of three potentiometric titrations.<sup>38</sup> The water content was determined *via* drying at 105 °C until a constant mass was obtained. All solvents and reagents were utilized as received without further purification. 1D and 2D NMR analyses were recorded at room temperature and a concentration of 20 mg  $\text{mL}^{-1}$  in 1 vol% d-TFA in  $\text{D}_2\text{O}$  on a 400 MHz Bruker Avance III HD NanoBay, equipped with 1H/BB z-gradient probe (BBO, 5 mm), nuclear magnetic resonance (NMR) spectrometer. All spectra were processed using TOPSPIN 3.6.5 and referenced directly ( $^1\text{H}$ ) or indirectly ( $^{13}\text{C}$ ) relative to an external 5 mM DSS standard in  $\text{D}_2\text{O}$ . NMR peak tables are available for all synthesized products within the ESI† or our previous publication.<sup>16</sup> Mechanochemical reactions were carried out in a MM400 vibratory ball milling system (manufactured by Retsch GmbH, Haan, Germany). Retsch GmbH supplied all ball and jar materials. IR spectra with a S/N-ratio of 30 000 : 1 were obtained from samples in neat form with a Quest ATR (Attenuated Total Reflectance) accessory with diamond crystal puck using a Shimadzu IRAFFINITY-1S Fourier Transform Infrared (FTIR) Spectrometer. The utilized equivalents were calculated based on the number of amine groups in a gram of material (5.27 mmol  $\text{g}^{-1}$ ).  $^{11}\text{B}$  NMR was utilized to verify the



absence of leftover boron salts in the products obtained *via* reductive amination.

### Relative molecular weight determination

The relative molecular weight to pullulan standards of the starting chitosan together with the obtained products was determined *via* LC/GPC ELSD. For the calibration curve, 1 mg of a pullulan standard (342 Da, 1 kDa, 6 kDa, 10 kDa, 50 kDa, 110 kDa, 200 kDa, 400 kDa and 800 kDa, PSS standards kit) was dissolved in 1 mL of an 0.1 vol% TFA aqueous solution to obtain a final concentration of 1 mg mL<sup>-1</sup>. For the chitosan samples, 5 mg of the sample was dissolved in 5 mL of a 0.1 vol% TFA aqueous solution to obtain a final concentration of 1 mg mL<sup>-1</sup>. All solutions were left overnight to equilibrate and filtered using a 25 mm polyethersulfone (PES) syringe filter (0.22 μm membrane) before injection. 20 μL was automatically injected into an Agilent 1260 Infinity II HPLC system equipped with PSS NOVEMA Max analytical linear M columns (10 μm particle size). A guard column and two GPC columns (8 × 300 mm) with a pore size of 100 Å, 3000 Å and 3000 Å were used respectively. The analyses were conducted at 25 °C with a flow rate of 0.5 mL min<sup>-1</sup>. Detection was done using an Agilent 1260 Infinity ELSD detector, the evaporation temperature was set at 80 °C and the nebulizer temperature was at 42 °C with an evaporator gas flow of 2.5 standard liters per minute (SLM). All raw data were directly processed *via* Matlab R2023b.<sup>39</sup>

### Determination of the degree of substitution (DS<sub>EA</sub>) *via* elemental analysis

Elemental analysis was performed using a Flash 2000 Elemental Analyzer (Thermo Fisher Scientific, Waltham, MA, USA) on 2 mg of each sample. For all samples, elements C, H, N, and S were measured (see Table S2†). 5-Bis(5-*tert*-butyl-benzoxazol-2-yl) thiophene (BBOT) was used as the standard reference. The degree of substitution was calculated *via* eqn (1).

$$\text{DS}_{\text{EA}} [\%] = \frac{M_{\text{C},\text{S}} - M_{\text{C},\text{chit}}}{n \times M_{\text{C}}} \times 100 \quad (1)$$

with  $M_{\text{C}}$  and  $M_{\text{N}}$  the molar masses of carbon and nitrogen,  $n$  the number of carbons of the added sidechain (8 for octanal and 10 for citronellal),  $M_{\text{C},\text{S}}$  the measured carbon/nitrogen ratio of the sample and  $M_{\text{C},\text{chit}}$  the measured carbon/nitrogen ratio of a blank sample only containing chitosan (see Table S2†).

### General procedure for the mechanochemical synthesis of *N*-alkylidene chitosan derivatives

Our previously optimized milling configuration (*e.g.* jar and ball material, milling frequency, amount of milling balls, size of milling balls, *etc.*) was employed without further optimization for this particular reaction.<sup>25</sup>

500 mg chitosan was added to a 25 mL SS jar containing two 15 mm SS balls. Next, either 0.125, 0.250, 0.5 or 1 eq. of aldehyde was added and the jar was sealed in place in a MM400 mixer milling system and milled at 30 Hz for either 10 minutes in the

case of 0.125 and 0.25 eq. and 30 or 40 minutes for 0.5 and 1 eq., respectively. Afterward, the obtained product was dispersed in 25 mL of EtOH, one drop of glacial acetic acid was added and the heterogeneous mixture was stirred for 30 minutes. Subsequently, the product was obtained *via* filtration, dried overnight in an oven at 60 °C and ground utilizing a mortar and pestle. All products were analyzed *via* FTIR and no traces of the aldehydes could be observed (see Fig. S1–S4 and S6†).

### Representative procedure for the mechanochemical synthesis of *N*-alkyl chitosan derivatives from *n*-alkyl aldehydes

Our previously optimized milling configuration (*e.g.* jar and ball material, milling frequency, amount of milling balls, size of milling balls, *etc.*) was employed without further optimization for this particular reaction.<sup>25</sup>

500 mg chitosan was added to a 25 mL SS jar containing two 15 mm SS balls. Next, 0.125 eq. of aldehyde was added and the jar was sealed in place in a MM400 mixer milling system and milled at 30 Hz for 10 minutes. Afterward, 10 mg of NaBH<sub>4</sub> (0.1 eq.) was added and the mixture was milled for another two hours. Next, the reaction mixture was left to cool down for one hour before continuing. Subsequently, the obtained product was dispersed in 10 mL of distilled water in a 50 mL centrifuge tube, a stirring bar was added and the mixture was stirred for five minutes. After five minutes, the product was centrifuged and filtered and the solid residue was washed with an additional 15 mL of distilled water. Next, the solid residue was dispersed in 25 mL of EtOH, one drop of glacial acetic acid was added and the heterogeneous mixture was stirred overnight. Subsequently, the product was obtained *via* filtration, dried overnight in an oven at 60 °C and ground utilizing a mortar and pestle. All samples were analyzed *via* <sup>11</sup>B NMR and FTIR and no traces of the aldehydes (see Fig. S7 and S8†) or boron signals could be observed.

### Representative procedure for the mechanochemical synthesis of *N*-alkyl chitosan derivatives from furfural and furfural-like aldehydes

Our previously optimized milling configuration (*e.g.* jar and ball material, milling frequency, amount of milling balls, size of milling balls, *etc.*) was employed without further optimization for this particular reaction.<sup>25</sup>

500 mg chitosan was added to a 25 mL SS jar containing two 15 mm SS balls. Next, 1 eq. of aldehyde was added and the jar was sealed in place in a MM400 mixer milling system and milled at 30 Hz for 30 minutes. Afterward, 100 mg of NaBH<sub>4</sub> (1 eq.) was added and the mixture was milled for another two hours. Next, the reaction mixture was left to cool down for one hour before continuing. Subsequently, the obtained product was dispersed in 10 mL of distilled water in a 50 mL centrifuge tube, a stirring bar was added and the mixture was stirred for five minutes. After five minutes, the product was centrifuged and the solid residue was dissolved in 10 mL 1% (v/v) acetic acid. Next, the solution was filtered through a cotton plug to remove insoluble material. Afterward, the cotton plug was rinsed with 5 mL of 1% (v/v) acetic acid. This solution was



concentrated down to about 5 mL. Subsequently, the product was precipitated with 50 mL of acetone and collected by centrifugation, dried overnight in an oven at 60 °C and ground utilizing a mortar and pestle. When the combined products of five runs were isolated only 50 mL of water, 65 mL of 1% (v/v) acetic acid and 100 mL acetone were required.

### Determination of the degree of substitution ( $DS_{\text{NMR}}$ ) via $^1\text{H}$ NMR analysis

The degree of substitution was determined *via* relative  $^1\text{H}$  NMR integration of the obtained compounds. For the *N*-octyl chitosan and the citronellal/chitosan amine adduct two detailed examples can be found in the ESI (see Fig. S22 and S23†). Additional information regarding the NMR characterization of these types of compounds can be found in our previous publication.<sup>16</sup>

### Green metrics calculation

The reaction mass efficiency (RME) (eqn (2)) and the process mass intensity (PMI) (eqn (3)) were calculated according to the best practices for sustainability metrics.<sup>40</sup> Detailed calculations can be found in the ESI.†

$$\text{RME} = \frac{\sum \text{total reactant mass that is attached on chitosan}}{\sum \text{total reactant mass}} \quad (2)$$

$$\text{PMI} = \frac{\sum \text{total process mass}}{\text{mass of isolated product}} \quad (3)$$

### Data availability

The data supporting this article have been included as part of the ESI.†

### Author contributions

Casper Van Poucke: conceptualization, methodology, formal analysis, investigation, data curation, writing – original draft, writing – review & editing, visualization, project administration, funding acquisition. Sven Mangelinckx: conceptualization, methodology, validation, resources, data curation, writing – review & editing, supervision. Christian V. Stevens: conceptualization, methodology, validation, resources, data curation, writing – review & editing, supervision, project administration, funding acquisition.

### Conflicts of interest

There are no conflicts to declare.

### Acknowledgements

The authors acknowledge the Research Board of Ghent University (BOF21/DOC/019) for funding. We gratefully

acknowledge Stef Ghysels for his help in acquiring the elemental analysis.

### References

- 1 C. Verma, M. A. Quraishi, A. Alfantazi and K. Y. Rhee, *Int. J. Biol. Macromol.*, 2021, **184**, 135–143.
- 2 X. Jin, J. Wang and J. Bai, *Carbohydr. Res.*, 2009, **344**, 825–829.
- 3 A. M. Omer, B. Y. Eweida, T. M. Tamer, H. M. A. Soliman, S. M. Ali, A. A. Zaatot and M. S. Mohy-Eldin, *Sci. Rep.*, 2021, **11**, 19879.
- 4 T. Fadida, A. Selilat-Weiss and E. Poverenov, *Food Hydrocolloids*, 2015, **48**, 213–219.
- 5 J. Lin, H. Meng, X. Guo, Z. Tang and S. Yu, *Foods*, 2023, **12**, 2921.
- 6 E. Bobu, N. Raluca, M. Lupei, F. L. Ciolacu and J. Desbrieres, *Cellul. Chem. Technol.*, 2011, **45**, 619–625.
- 7 N. Mati-Baouche, C. Delattre, H. de Baynast, M. Grédiac, J.-D. Mathias, A. V. Ursu, J. Desbrières and P. Michaud, *Molecules*, 2019, **24**, 1987.
- 8 I. Demir-Yilmaz, M. S. Ftouhi, S. Balayssac, P. Guiraud, C. Coudret and C. Formosa-Dague, *Chem. Eng. J.*, 2023, **452**, 139349.
- 9 O. Guaresti, C. García-Astrain, T. Palomares, A. Alonso-Varona, A. Eceiza and N. Gabilondo, *Int. J. Biol. Macromol.*, 2017, **102**, 1–9.
- 10 M. Huo, Y. Zhang, J. Zhou, A. Zou, D. Yu, Y. Wu, J. Li and H. Li, *Int. J. Pharm.*, 2010, **394**, 162–173.
- 11 J. Desbrières, C. Martinez and M. Rinaudo, *Int. J. Biol. Macromol.*, 1996, **19**, 21–28.
- 12 M. Yalpani and L. D. Hall, *Macromolecules*, 1984, **17**, 272–281.
- 13 V. Isoni, K. Mendoza, E. Lim and S. K. Teoh, *Org. Process Res. Dev.*, 2017, **21**, 992–1002.
- 14 K. Novak, M. J. Cupp and T. S. Tracy, in *Dietary Supplements: Toxicology and Clinical Pharmacology*, ed. M. J. Cupp and T. S. Tracy, Humana Press, Totowa, NJ, 2003, pp. 33–39.
- 15 J. Hu, Z. Huang and Y. Liu, *Angew. Chem., Int. Ed.*, 2023, **62**, e202306999.
- 16 C. Van Poucke, E. Verdegem, S. Mangelinckx and C. V. Stevens, *Carbohydr. Polym.*, 2024, **337**, 122131.
- 17 M. A. Mohamed, J. Jaafar, A. F. Ismail, M. H. D. Othman and M. A. Rahman, in *Membrane Characterization*, ed. N. Hilal, A. F. Ismail, T. Matsuura and D. Oatley-Radcliffe, Elsevier, 2017, pp. 3–29.
- 18 L. Marin, B. Simionescu and M. Barboiu, *Chem. Commun.*, 2012, **48**, 8778–8780.
- 19 J. W. Lee, J. Park, J. Lee, S. Park, J. G. Kim and B.-S. Kim, *ChemSusChem*, 2021, **14**, 3801–3805.
- 20 S. Kalliola, E. Repo, V. Srivastava, F. Zhao, J. P. Heiskanen, J. A. Sirviö, H. Liimatainen and M. Sillanpää, *Langmuir*, 2018, **34**, 2800–2806.
- 21 N. Pétry, T. Vanderbeeken, A. Malher, Y. Bringer, P. Retailleau, X. Bantreil and F. Lamaty, *Chem. Commun.*, 2019, **55**, 9495–9498.



- 22 V. Canale, M. Kamiński, W. Trybała, M. Abram, K. Marciniak, X. Bantreil, F. Lamaty, J. R. Parkitna and P. Zajdel, *ACS Sustain. Chem. Eng.*, 2023, **11**, 16156–16164.
- 23 V. Duhan, S. Yadav, C. Len and B. Lochab, *Green Chem.*, 2024, **26**, 483–497.
- 24 X. Chen, H. Yang, Z. Zhong and N. Yan, *Green Chem.*, 2017, **19**, 2783–2792.
- 25 C. Van Poucke, A. Vandeputte, S. Mangelinckx and C. V Stevens, *Green Chem.*, 2023, **25**, 4271–4281.
- 26 H. C. B. Paula, R. B. C. Silva, C. M. Santos, F. D. S. Dantas, R. C. M. de Paula, L. R. M. de Lima, E. F. de Oliveira, E. A. T. Figueiredo and F. G. B. Dias, *Int. J. Biol. Macromol.*, 2020, **163**, 1591–1598.
- 27 M. Montiel-Herrera, A. Gandini, F. M. Goycoolea, N. E. Jacobsen, J. Lizardi-Mendoza, M. Recillas-Mota and W. M. Argüelles-Monal, *Carbohydr. Polym.*, 2015, **128**, 220–227.
- 28 L. Vugrin, M. Carta, F. Delogu and I. Halasz, *Chem. Commun.*, 2023, **59**, 1629–1632.
- 29 F. Parenti, F. Tassinari, E. Libertini, M. Lanzi and A. Mucci, *ACS Omega*, 2017, **2**, 5775–5784.
- 30 S. Maity, N. Naskar, B. Jana, S. Lahiri and J. Ganguly, *Carbohydr. Polym.*, 2021, **251**, 116999.
- 31 C. Hansch, A. Leo and R. W. Taft, *Chem. Rev.*, 1991, **91**, 165–195.
- 32 A. Sela, E. Cohen, L. Avram, V. Rodov and E. Poverenov, *Green Chem.*, 2023, **25**, 922–927.
- 33 J. P. Adams, C. M. Alder, I. Andrews, A. M. Bullion, M. Campbell-Crawford, M. G. Darcy, J. D. Hayler, R. K. Henderson, C. A. Oare, I. Pendrak, A. M. Redman, L. E. Shuster, H. F. Sneddon and M. D. Walker, *Green Chem.*, 2013, **15**, 1542–1549.
- 34 D. Prat, A. Wells, J. Hayler, H. Sneddon, C. R. McElroy, S. Abou-Shehada and P. J. Dunn, *Green Chem.*, 2016, **18**, 288–296.
- 35 R. R. A. Bolt, J. A. Leitch, A. C. Jones, W. I. Nicholson and D. L. Browne, *Chem. Soc. Rev.*, 2022, **51**, 4243–4260.
- 36 T. A. Akopova, T. N. Popyrina and T. S. Demina, *Int. J. Mol. Sci.*, 2022, **23**, 10458.
- 37 M. Lavertu, Z. Xia, A. N. Serreqi, M. Berrada, A. Rodrigues, D. Wang, M. D. Buschmann and A. Gupta, *J. Pharm. Biomed. Anal.*, 2003, **32**, 1149–1158.
- 38 H. Wang, C. Qian and M. Roman, *Biomacromolecules*, 2011, **12**, 3708–3714.
- 39 H. G. B. Sadao Mori, *Size Exclusion Chromatography*, Springer-Verlag Berlin Heidelberg, 1999.
- 40 D. P. Debecker, K. Kuok (Mimi) Hii, A. Moores, L. M. Rossi, B. Sels, D. T. Allen and B. Subramaniam, *ACS Sustain. Chem. Eng.*, 2021, **9**, 4936–4940.
- 41 G. Yang, S. Régner, N. Huin, T. Liu, E. Lam and A. Moores, *Green Chem.*, 2024, **26**, 5386–5396.

